Functional insights from targeted imaging BACE1: The first near-infrared fluorescent probe for Alzheimer's disease diagnosis

Anyao Bi
Xiangya School of Pharmaceutical Sciences, Central South University
Junyong Wu
Department of Pharmacy the second Xiangya Hospital, Central South University
Shuai Huang
Xiangya School of Pharmaceutical Sciences, Central South University
Yongjiang Li
Department of Pharmacy the second Xiangya Hospital, Central South University
Fan Zheng
Xiangya School of Pharmaceutical Sciences, Central South University
Jipeng Ding
Xiangya School of Pharmaceutical Sciences, Central South University
Jie Dong
Xiangya School of Pharmaceutical Sciences, Central South University
Daxiong Xiang
Department of Pharmacy the second Xiangya Hospital, Central South University
Wenbin Zeng (wbzeng@hotmail.com)
Xiangya School of Pharmaceutical Sciences, Central South University

Research Article

Keywords: Alzheimer's disease, Fluorescent probe, Near-infrared fluorescence imaging, BACE1, Nanomaterials

Posted Date: May 18th, 2022

DOI: https://doi.org/10.21203/rs.3.rs-1642706/v1

Abstract

Background

β-Secretase (BACE1) is the vital enzyme in the pathogenic processes of Alzheimer's disease (AD). However, the development of a powerful tool with sensitivity for BACE1 determination in vivo is a challenge.

Methods

A novel NIR fluorescent probe **HBAE** was synthetized starting from 2-hydroxy-3-methylbenzaldehyde and 2-amino-benzenethiol via five steps. The fluorescence mechanism in the ESIPT systems of **HBAE** was insighted studied with time-dependent density functional theory (TD-DFT) at the TDPBE0 level with the def2-TZVP approach. The corresponding docking between **HBAE** and BACE1 (PDB: 5I3Y) was performed through the ducking method by DOCK6.8. Then the BBB permeability of **HBAE** is verified by transwell orifice plate. 5XFAD mice and age-matched wild-type mice were employed to observe the brain kinetics by intravenous injection. Finally, immunohistochemistry was performed on the AD brain section to reveal the levels of BACE1 in hippocampus and cortex areas and other regions in AD mice through the brain tissue slices by **HBAE**.

Results

The novel NIR fluorescent probe was self-assembly to nanomaterial and subsequently was successfully applied in imaging BACE1 in AD model mice. The capability of **HBAE** in reflecting different level of BACE1 was performed by the specific imaging of the hippocampus region.

Conclusions

We reported the first ESIPT near-infrared fluorescence material for monitoring endogenous BACE1 in the AD live model mice, thus offering a versatile chemical tool for visualizing in the pathological processes of AD live brains. Remarkably, high resolution images showed the localization of red fluorescence stains in hippocampus of the AD brain. This study provides a promising way for functional insights from protein BACE1 in vivo.

1. Introduction

As one of the progressive neurodegenerative disorders in brain, Alzheimer’s disease (AD) has been regarded as an incurable condition [1–5]. Among various biomarkers, the formation and progressive accumulation of amyloid-β (Aβ) plaques in the brain is considered as an important pathological hallmark for diagnosis of AD at early stage [6–12]. Although thioflavin derivatives (ThT or ThS) are commercially

available for in vitro histological staining amyloid fibrils [13–17], several inherent defects (e.g. distorted signals from fluorescence quenching effect at high concentration, inevitable noises from “always-on” mode, and poor blood-brain barrier (BBB) penetrability largely hinder their further application in in vivo imaging [18–20]. In fact, it is still far from accurate feedback for in situ visualization of Aβ plaques.

Generally, the Aβ peptide monomer is generated through the proteolysis of amyloid precursor protein (APP) by two typical proteases, β-secretases and γ-secretases. Upon cleavage of APP by β-secretases, a soluble extracellular fragment (sAPPβ) is generated, and then its cell membrane-bound fragment (C99) undergoes a cleavage catalyzed by γ-secretase to form the Aβ monomer. As such, inhibiting the activity of β-secretases open a new window to limit the production rate of Aβ in vivo. In this way, β-secretase, also termed β-site APP-cleaving enzyme 1 (BACE1), shows a great significance in AD progression and provides a vital therapeutic target toward AD diagnosis and treatment.

To date, only a few fluorescent probes have been designed for detection of BACE1. For example, Franz et al. reported a probe based on fluorescence resonance the activities of energy transfer (FRET), allowing real time monitoring of the levels of BACE1 [21]. It was constructed through connecting DMACA with DABCYL quencher by a substrate of BACE which had a broad absorbance peak at 420–520 nm but faint fluorescence emission. Upon exposure to BACE1, by which the DABCYL quencher was removed, resulted in the fluorescence recovery of fluorophore DMACA. Tian’s group reported another two-photon fluorescent probe for BACE1 based on FRET as well[22]. The probe consists of an energy donor (mCyd) and an energy acceptor (AF633) conjugated by a peptide spacer which simultaneously behaves as a substrate of BACE1. Under the effect of BACE1, the signals of the probe changed from the fluorescence of AF633 to that of mCyd due to the separation of FRET donor–acceptor pair. Such a system is the first reported two-photon ratiometric fluorescent probe for imaging of BACE1 in living objects. However, NIR material for BACE1 detection that can be permeable into blood-brain barrier are still quite rare nowadays.

Aggregation-induced emission (AIE) is a preferential method to design probes for the identification of protein fibrillogenesis, particularly account of its fluorescence emssion is so associated with the binding behavior during the aggregation process [23, 24]. Nevertheless, the redundant hydrophobic aromatic rings in such AIE probes and the additional π-conjugated bridge introduced to extend the emission wavelength to the NIR region, would undergo unwanted initial aggregation before binding toward BACE1, inevitably leading to a “false-positive” fluorescence signal. Hence, it is urgent to overcome the dilemma which is to balance the lipophilic requirement for facilitating longer emission wavelength with the docking behavior from water to protein detection of BACE1. In this paper, we increased the water solubility of the AIE probes which have NIR emision nanomaterials to obtain a favorable miscibility in aqueous media, thus affording the fluorescence imaging of BACE1 with high sensitivity and fidelity. We envisioned that the integration of deep penetration characteristic and tunable light-up fluorescence in such NIR AIE-active probes could gain unprecedented progress to directly visualize BACE1 deposition in vivo. Except for the difficulties mentioned above, photobleaching, tissue autofluorescence, and the detailed probes concentration will also cause a certain amount of background signals such as blood and tissue, which makes the fluorescent imaging working only on single short wavelength channel not reliable. While the excited state

intramolecular proton transfer (ESIPT) is an important mechanism for constructing ratiometric fluorescent probes which might be a solution to the predicament. Besides, ESIPT has received other considerable attention due to its large Stokes shifts, intensive absorption and emission in the UV/VIS region, and dual emission behaviour.

Under this circumstance, we develop a novel NIR fluorescent probe **HBAE** ((Z)-4-(4-(2-(3-(benzo[d]thiazol-2-yl)-4-hydroxy-5-methylphenyl)-1-cyanovinyl)phenyl)-1-methylpyridin-1-ium) based on the mechanism of AIE and ESIPT to image BACE1 in vitro and in vivo. A lipophilic π-conjugated benzene-bridge is conjugated to the ESIPT nuclear parent to extend the emission to NIR wavelength range. Then **HBAE** is obtained by the connection of pyridinium to the benzene-bridge. Consequently, the target of meeting the lipophilic requirement for extending the emission wavelength and avioding a “background-positive” fluorescent signal in BACE1 imaging is realized with our probe. In vitro and in vivo experiments have provided evidences of the accurate imaging of intracellular BACE1. The imaging capacity of the probe towards BACE1 is firstly approved in cells. Then the BBB permeability of **HBAE** is verified before the in vivo assays. The feasibility of the probe is futher confirmed in the 22-month-old male AD-model mice. Finally, the result that the activities of BACE1 in hippocampus and cortex areas is higher than those in other regions in AD mice is intuitively shown through the brain tissue slices by **HBAE**. It is hoped that **HBAE** can serve as an efficient alternative to the NIR AD probes and provide a robust sensing nanomaterial platform to investigte the role of BACE1 in the pathogenesis of AD. Herein, we reported the first ESIPT near-infrared fluorescence probe for monitoring endogenous BACE1 in the AD live brains, and provided a versatile chemical tool for visualizing the pathological process of AD and its diagnosis.

2. Methods

2.1. Materials

All chemicals and reagents were used as received useless otherwise specified. Vitamin B1, benzaldehyde, and *p*-chloroaniline (99.5%) were purchased from Energy Chemical Co., Ltd (China). 4-Pyridine carboxaldehyde (98%) and pyridine were purchased from Sinopharm Chemical Reagent Co., Ltd (China). 4’,6-diamidino-2-phenylindole (DAPI) were purchased from Sigma-Aldrich. The high sugar DMEM base used was purchased from Thermo Fisher technology, phosphate buffered saline (PBS) were purchased from Invitrogen. The cell counting kit-8 (CCK-8) cytotoxicity assay kit was a commercial product of Beyotime Biotechnology (China). Milli-Q water was supplied by Milli-Q Plus System (Millipore Corporation, United States). The 22-month-old 5XFAD mice and wild-type mice were ordered from the Jackson Laboratory (34840), and maintained under standard conditions. Cell lines: derived Endothelial cells.3 (bEnd.3) and N2a, HEK293, U87-MG were continuously cultured in the Second Xiangya Hospital laboratory.

2.2. Synthesis

The probe **HBAE** was synthetized from 2-hydroxy-3-methylbenzaldehyde and 2-amino- benzenethiol by 5 steps. After Duff reaction and Suzuki reaction, the probe was given 0.32 g of yellow solid powder was

obtained with a total yield of 19.2%. ^{1}H NMR (500 MHz, DMSO-d6, δ): 9.05(s, 1H), 8.03–8.09(d, 2H), 7.70–7.71 (d, H), 7.63 (s, H), 7.59(d, H), 7.58–7.55 (d, 2H), 7.51–7.45 (d, 2H), 7.41–7.39 (d, 2H), 7.32–7.30 (d, 2H), 7.22 (d, H), 7.18–7.14 (d, H), 4.03 (s, 3H), 1.34 (s, 3H). ^{13}C NMR (125 MHz, DMSO-d6): δ): 168.35, 155.45, 153.58, 153.46, 151.47, 151.31, 146.17, 146.11, 144.10, 143.95, 137.96, 137.92, 134.02, 133.87, 133.18, 133.14, 129.31, 129.25, 127.67, 127.57, 127.04, 126.56, 124.46, 124.42, 123.01, 122.62, 118.50, 117.07, 47.40, 16.36. Mass spectrometry (ESI-MS, m/z): $[M]^+$ Calcd. for $[C_{29}H_{22}N_3OS]^+$ 460.1515; found 460.1449.

2.3. Establishment of blood-brain barrier in vitro

Transwell orifice plate was used in the experiment. 10000 bend. 3 cells were inoculated into each well in the upper chamber. Complete culture medium was added into the lower chamber, and the solution was changed every 48 hours. The resistance was measured by trans endothelial resistance meter (TEER). When the resistance value was greater than 200 Ω / cm^2, the in vitro blood-brain barrier was successfully established. U87-MG cells were inoculated into the lower chamber, adhered to the wall overnight, and **HBAE** were added into the upper chamber after 1, 2 and 4 hours respectively, the lower ventricular cells were fixed with paraformaldehyde, washed with PBS for three times, and stained with DAPI staining solution. After washing with PBS for three times, the BBB ability of the probe was observed under fluorescence microscope.

3. Results And Discussion

3.1.Molecular design and insighted fluorescence mechanism

It is due to the cellular localization of the active BACE enzyme that inhibitors fail in their attempts to inhibit cellular activity. When exposed to an extracellular environment, BACE is inactive at pH 7.4, so may not cause the cleavage of APP. A pH value of four to five is required for BACE1 to acquire activity once it is endocytosed to an endosome[11]. BACE1 cannot be inhibited by inhibitors that cannot access these endosomal compartments. Due to limited accessibility to intracellular vesicles, conventional FRET probes are ineffective as well for monitoring BACE1 activity in vitro.

Fluorophore's molecular design and on achieving excitation coefficients and optimal excitation/emission spectra have attracted an increasing experimental interest, but few efforts are devoted to fundamental mechanistic studies. In this paper, we in-sighted the fluorescence mechanism in the ESIPT systems of **HBAE** probe with the ideal quantum chemical tools. Using time-dependent density functional theory (TD-DFT), we explore the potential energy surfaces (PESs) of the lowest-lying excited states rather than analysing frontier orbital energy diagrams and performing ESIPT thermodynamics calculations and the radiative and nonradiative decay rates from the involved excited states are computed from first-principles using a thermal vibration correlation function formalism [25, 26]. With such strategies, our results reveal the real origins of the fluorescence intramolecular proton transfer.

The emission mechanism of these fluorescence plays an important role in the molecular design and construction of a functional system. We simulated three possible nonradiative decay channels from the S1-state Franck − Condon structure of Z-enol, then consuming its excited-state energy and the ESIPT process along the O − H distances from Z-keto*. The PBE0/Def2-TZVP optimized S1-MEPs, are shown in Fig. 1. The computational results indicate that the probe being excited to the S1 state, a nonradiative decay from the excited to the ground state was observed and barrierless ESIPT from enol to keto tautomer in the waterable solution.

According to the reported structure, Our calculations confirm Z-enol as the most stable configuration in the S0 state at the PBE0 level. we calculated configurations of HBT the vertical absorption energy at Z-enol including Z-keto, E-enol, and E-keto to predict its absorption spectra. The S0 → S1 excitation leading to a spectroscopically bright state with π − π* character, mainly results from the HOMO to LUMO excitation. The S0 → S1 vertical excitation energy calculated is 540 nm (3.85 eV, f = 0.46) by TD-PBE0 with def2-TZVP approach. Both of those results are in agreement to 540 nm the experimentally measured absorption maximum (Figure S1).

The tautomerized product, Z-keto*, shows vertical emission energy of 650 nm (2.53 eV) at the TDPBE0 level with the def2-TZVP approach (650 nm, 2.50 eV with SS-PCM calculation), which is in excellent agreement with the experimentally fluorescence maximum of 650 nm. Therefore, Z-keto* is assigned as the most likely emissive structure on the S1 state. In short, using the electronic-structure calculations in combination with the TDPBE0 level with the def2-TZVP approach, we have comprehensively investigated the possible emission channels of **HBAE**, thus confirming that fluorescence emission is owing to the effect of the ESIPT and subsequent bond-rotation relaxation, both of which are essential.

3.2. Mechanism studies

Inspired by the prominent fluorescent performances of **HBAE** towards neuro cells, we were then unveiled the underlying mechanism of the probe specificity and activity. According to previous reports, the effects of many brain-targeting compounds are attributed to the strong and selective inhibition of BACE1.[3, 5, 19] Thus, we hypothesized that the reason of the strong affinity of **HBAE** on neuro cells probably was the strong targeting binding of it towards BACE1, by which the probe ultimately achieved specific target of neuro cells. In other words, as well demonstrated above that the probe could perform neuro cells specific bio-imaging, we conclused that the intracellular fluorescence intensity should be highly associated with the content of BACE1, and it in turn could signal the location of the targeting BACE1.

To prove our thoughts, the corresponding docking between **HBAE** and BACE1 (PDB: 5I3Y) was carried out initially. It was performed through the ducking method by swiss predict. As depicted in Fig. 2A, the benzene ring on benzothiazole had Van der Waals force with Thr72 and Gln73, while the benzene-bridge had the same interaction with Val309. It was shown that **HBAE** was inserted into a nonpolar binding cavity of BACE1. It was further reflected that the fragments of the hydroxyl group and the cyano group of the probe were docked into the catalytic site of BACE1. These groups were interacted with Ser325 and

Lys321 through hydrogen bonds, respectively. Besides, the N atom on benzothiazole also had a strong hydrogen bond with the amino acid residues of BACE1, including Gln73 and Thr 232 in Fig. 2B. These results suggested that the targeting ability of **HBAE** towards neuro cells could be based on the specific binding between the probe and BACE1.

3.3. Specific imaging of BACE1 in human and mouse cells

Since BACE1 in different human and mouse cell lines (HEK293 is a human embryonic kidney cell, U87-MG is a human glioma cell, N2a and bEnd. 3 are mouse derived cells) was analyzed using western blot images. As shown in Figure. S5., BACE1 contents obviously increased in N2a, HEK293, U87-MG and bEnd.3, which is the component part of the blood-brain barrier. These results demonstrated that the levels of BACE1 were highly expressed in the four cell lines. Binding affinity was another important factor for probes to imaging the BACE1. After the addition of **HBAE** to the BACE1, it was self-assembled to form nanomaterial and the corresponding NIR fluorescence enhancement was immediately found at 665 nm, demonstrating that **HBAE** showed specific binding affinity with BACE1. So, the highly sensitive NIR fluorescence response of **HBAE** with BACE1 made it promising nanomaterials for mapping BACE1 in AD mouse brain.

To detect and image BACE1 in the four cell lines, the four cells were stained with DAPI, **HBAE** and BACE1 specific antibody followed by the treatment with fluorescently (Alex fluo 488) labeled secondary antibody, and the images were captured under the fluorescence microscope (Fig. 3). Staining with Alex 488-BACE1, a specific antibody of BACE1, the green fluorescence is observed in the four cells. BACE1 is incubated with primary antibody binding and then decolored with green secondary antibody(Alex fluo 488), so green fluorescence represents BACE1, which is highly expressed in four cell lines (Fig. 3). These results revealed that the four cell lines all have the high levels of BACE1, and **HBAE** can also be well imaged on cells and overlapped with BACE-1 specific antibody fluorescence. it provides a basis for the **HBAE** probe qualified endogenous BACE1 detection in human and mouse brain cells.

Next, for imaging and sensing of endogenous BACE1 in live human and mouse cells, 5.0 μM **HBAE** probe was incubated with cells for 20 min. From Fig. 4, we can see that the probe successfully entered into the human and mouse cells as shown in the overlay channel, the probe **HBAE** can be obvious observed from the merge image that it is well colocated with Alex fluo 488, indicating it can target BACE1 protein. The images obtained from the four cells showed green fluorescence signal which confirmed the presence of BACE1 mainly in the cell membrance and cytoplasm (Fig. 4), and demonstrating that the developed **HBAE** probe was quite qualified for endogenous BACE1 detection as expected.

3.4.Evaluation of the blood brain barrier permeability

Having confirmed BACE1 specific NIR light-up responses in BACE1 highly expressed cells. we further comfirmed of the probe is proved by simulating the blood-brain barrier in vitro with Transwell plate. The bEnd. 3 cells planted in the upper chamber to simulate the blood-brain barrier in vitro, and then U87-MG cells are planted in the lower chamber. It can be found that within four hours, strong fluorescence could

be captured in U87-MG cells indicating that **HBAE** can cross smoothly and has good permeability, the fluorescence staining diagram that the staining effect of U87-MG cells in the lower layer is obvious, indicating that the probe can penetrate the in vitro BBB model. The Transwell experiment analysis further confirmed that **HBAE** showed ideal permeability (Fig. 5). and realize the staining of lower cells, indicative of its potential for matching BBB penetrability. It provides ideal results for HBAE further imaging in living animals. In fact, via intravenous injection of **HBAE** (perfused with PBS), respectively, high-resolution imagine from the brain homogenate extraction of wild-type mice could be obtained to verify the BBB penetrability (Fig. 6).

3.5. In vivo imaging in the AD model

As shown in Fig. 6A, 22-month-old male AD-model (5XFAD) mice and age-matched wild-type mice were employed to observe the brain imaging by intravenous injection, to further confirm the practicability of **HBAE** for in vivo imaging BACE1. The strong fluorescence signals were observed in the brain position. In particular, the fluorescence intensity of **HBAE** in the brain regions of the AD-model mice was much higher than that in the control of wild-type mice at 120 min after postinjection, there is strong fluorescence at 2 h, and the fluorescence will be stronger with time lapse, and there is always a strong fluorescence at 24 h. In contrast, in wild-type mice, the fluorescence became very weak after 24 hrs indicative of specifically trapping BACE1 in vivo with probe **HBAE**. In addition, the cell viability of the probe **HBAE** by the CCK8 assays demonstrated its lower toxicity (Figure S6 in the Supporting Information). As shown in Fig. 6B, the fluorescent image of ex vivo brain of AD-model mice was obviously higher than that in the wild-type mice at corresponding time. As shown in Fig. 6C and D, the results indicated that **HBAE** could cross the blood–brain barrier and image BACE1 in vivo.

Ex vivo histology of **HBAE** binding to BACE1 in AD mice was carried out to further confirmed the in vivo performance. After 120 min of intravenous injection of **HBAE**, a higher number of fluorescence was observed in the mouse brain,liver and kidney,indicating the probe mainly distribution in these organs. It was further confirmed that the in vivo fluorescence signal was resulting from **HBAE** specifically binding to BACE1.

3.6. In vitro imagine of the hippocampus region in AD

It is well-known that the areas of the brain such as the hippocampus and cortex, that are primarily involved in memory processing, are likely to be first affected by AD memory loss. Immunohistochemistry was performed on the AD brain section to see which part had high expression of BACE1, from the experimental results in Figure.8A it can be seen that the levels of BACE1 in hippocampus and cortex areas were higher than those in other regions in AD mice. The images under red fluorescence channel revealed that the probe **HBAE** can well target proteins in AD mouse brain slices.

Next, the microscope images of the hippocampus region in AD mouse brain tissue labelled with the synthesized probe were obtained. After 120 min of intravenous injection of **HBAE**, the brain slice was obtained and incubated with BACE1 antibody, staining with secondary antibody, and finally stain the nucleus, a higher number of BACE1 were observed in the brain slices from 5XFAD mice (Fig. 8). As shown

in Fig. 8B the probe **HBAE** showed the excellent colocalization of BACE1 during staining the same section with BACE1 antibody (5.0 μM) was subsequently used for evaluating the levels of BACE1 in AD (5XFAD) mouse brain tissues. Figure 8B illustrates different regions of the mouse brain slice, such as field of hippocampus. From Fig. 8B, the pseudocolor of the Fgreen/Fred channel changed from green to red in the regions hippocampus and their arounds, demonstrating that BACE1 in these regions of AD mouse brain was higher than other regious. As shown in Fig. 8A, BACE1 obviously stained in hippocampus areas by BACE1-antibody, compared with those in other areas in AD mouse brain. As shown in Fig. 8B, **HBAE** could well staining the highly expressed BACE1 in the hippocampus area after entering the mouse. These results demonstrated that the levels of BACE1 were nonuniform in different regions of AD mouse brain. From the experimental results in Fig. 8, the mapping of fluorescent imaging of BACE1 in hippocampus and cortex areas was obviously beyond regions in AD mice, which can be regarded as that BACE1 levels were closely related to the pathogenesis of AD.

4. Conclusion

In summary, we reported the first ESIPT near-infrared fluorescence probe of monitoring endogenous BACE1 in the AD live brains, thus offering a promising chemical tool for visualizing in the pathological processes of AD live brains. In vitro and in vivo experiments provided ideal results of the accurate detection and mapping of BACE1. The first time NIR emission BACE1 was observed specificity, making a breakthrough in detection of BACE1 in vivo. The probe **HBAE** exhibited remarkable binding affinity with BBB penetrability, and high-performance NIR emission. The novel near-infrared nanomaterial was successfully applied for imaging and sensing of BACE1 in live cells, AD brain tissues and AD mice in vivo for the first time. Remarkably, high resolution images showed the localization of green fluorescence around red fluorescence stains in both hippocampus and cortex regions of the AD brain. This study provides an efficient alternative to the commercial probes serving a promising way for the imaging BACE1 by NIR nanomaterial and a new pathway for insights into protein BACE1 in vivo.

Declarations

Author contributions

Wenbin Zeng and Daxiong Xiang conceived and supervised the project. Anyao Bi and Junyong Wu contributed to the experimental designs, performed experiments, analyzed data, interpreted the results and wrote the original manuscript; Shuai Huang, Yongjiang Li, Fan Zheng, Jipeng Ding performed experiments; Wenbin Zeng and Jie Dong critically revised the manuscript. All authors contributed and reviewed the results and approved the final manuscript.

Funding

This work was supported by the financial supports from National Natural Science Foundation of China (81971678 and 81671756), Science and Technology Foundation of Hunan Province (2020SK3019,

2019SK2211 and 2019GK5012), and the Innovation Fund for Postgraduate Students of Central South University (2019zzts770), and the Fundamental Research Funds for the Central Universities of Central South University (2018zzts041, 2018dcyj067).

Availability of data and materials

The datasets used and/or analyzed in this study are available from the corresponding author on reasonable request.

Ethics approval and consent to participate

The animal experiment was approved by the Animal Ethics and welfare Committee, at the Second Xiangya Hospital, Central South University (No.2021595). All animal studies were carried out using the Institutional Animal Care and Use Committee (IACUC) approved procedures.

Consent for publication

All authors read and approved the final manuscript.

Conflict of interest

The authors declare no conflict of interest.

References

1. Hardy J, Selkoe D. The amyloid hypothesis of Alzheimer's disease: progress and problems on the road to therapeutics. Science. 2002; 297: 353–60.
2. Ibrahim M, Gabr M. Multitarget therapeutic strategies for Alzheimer's disease. Neural Regener Res. 2019; 3: 437–40.
3. Evin G, Barakat A, Masters C. BACE: Therapeutic target and potential biomarker for Alzheimer's disease. Int J Biochem Cell Biol. 2010; 42: 1923–6.
4. Martin L, Latypova X, Wilson C, Magnaudeix A, Perrin M, Yardin C, Terro F. Tau protein kinases: involvement in Alzheimer's disease. Aging Res Rev. 2013; 12: 289–309.
5. Postina R. A closer look at alpha-secretase. Curr Alzheimer Res. 2008; 5: 179–86.
6. Bailey R, Covy J, Melrose H, Rousseau L, Watkinson R, Knight J, Miles S, Farrer MJ, Dickson DW, Giasson BI, Lewis J. LRRK2 phosphorylates novel tau epitopes and promotes tauopathy. Acta Neuropathol. 2013;126: 809–27.
7. Zhao J, Lu W, Ren Y, Fu Y, Martens Y, Shue F, Davis MD, Wang X, Chen K, Li F, Liu CC, Graff-Radford NR, Wszolek ZK, Younkin SG, Brafman DA, Ertekin-Taner N, Asmann YW, Dickson DW, Xu Z, Pan M, Han X, Kanekiyo T, Bu G. Apolipoprotein E regulates lipid metabolism and α–synuclein pathology in human iPSC–derived cerebral organoids. Acta Neuropathol. 2021; 142: 807–25.

8. Erskine D, Koss D, Korolchuk V, Outeiro T, Attems J, McKeith I. Lipids, lysosomes and mitochondria: insights into Lewy body formation from rare monogenic disorders. Acta Neuropathol. 2021;141: 511–26.
9. Mancini F, De Simone A, Andrisano V. Beta-secretase as a target for Alzheimer's disease drug discovery: an overview of in vitro methods for characterization of inhibitors. Anal Bioanal Chem. 2011; 400: 1979–96.
10. Jordan J, Whittington D, Bartberger M, Sickmier E, Chen K, Cheng Y, Judd T. Fragment-linking approach using (19)F NMR spectroscopy to obtain highly potent and selective inhibitors of β-Secretase. J Med Chem. 2016; 59: 3732–49.
11. Savelieff M, Nam G, Kang J, Lee H, Lee M, Lim M. Development of multifunctional molecules as potential therapeutic candidates for Alzheimer's disease, Parkinson's disease, and amyotrophic lateral sclerosis in the last decade. Chem Rev. 2019; 119: 1221–322.
12. Ghosh A, Brindisi M, Yen Y, Cardenas E, Ella-Menye J, Kumaragurubaran N, Huang XP, Tang J, Mesecar AD. Design, synthesis, and X-ray structural studies of BACE-1 inhibitors containing substituted 2-oxopiperazines as P1'-P2' ligands. Bioorg Med Chem Lett. 2017; 27: 2432–38.
13. Zhang D, Peng R, Liu W, Donovan M, Wang LL, Ismail I, Li J, Li J, Qu FL, Tan WH. Engineering DNA on the surface of upconversion nanoparticles for bioanalysis and therapeutics, ACS Nano. 2021; 15: 17257–74.
14. Xie S, Ai LL, Cui C, Fu T, Cheng XD, Qu FL, Tan WH. Functional aptamer-embedded nanomaterials for diagnostics and therapeutics. ACS Appl Mater Interfaces. 2021; 13: 9542–60.
15. Lo C, Lim C, Ding Z, Wickramasinghe S, Braun A, Ashe K, Rhoades E, Thomas DD, Sachs JN. Targeting the ensemble of heterogeneous tau oligomers in cells: A novel small molecule screening platform for tauopathies. Alzheimer’s Dementia. 2019; 15: 1489–502.
16. Wang SS, Liu ZK, Liu JJ, Cheng Q, Wang Y, Liu Y, Ni W, Chen H, Song M. Imaging asparaginyl endopeptidase (AEP) in the live brain as a biomarker for Alzheimer’s disease. J Nanobiotechnol.2021; 19, 249–67.
17. Zhu F, Tan G, Zhong Y, Jiang Y, Cai L, Yu ZQ, Liu S, Ren F. Smart nanoplatform for sequential drug release and enhanced chemo-thermal effect of dual drug loaded gold nanorod vesicles for cancer therapy. J Nanobiotechnol. 2019; 17: 44–59.
18. Salado I, Redondo M, Bello M, Perez C, Liachko N, Kraemer B, Miguel L, Lecourtois M, Gil C, Martinez A, Perez DI. Protein kinase CK-1 inhibitors as new potential drugs for amyotrophic lateral sclerosis. J Med Chem. 2014;57: 2755–72.
19. Yue Y, Huo F, Ning P, Zhang Y, Chao J, Meng X, Yin CX. Dual-site fluorescent probe for visualizing the metabolism of Cys in living cells, J Am Chem Soc. 2017; 139: 3181–5.
20. Han S, Ma W, Jiang D, Sutherlin L, Zhang J, Lu Y, Huo N, Chen Z, Engle JW, Wang Y, Xu X, Kang L, Cai W, Wang L. Intracellular signaling pathway in dendritic cells and antigen transport pathway in vivo mediated by an OVA@DDAB/PLGA nano-vaccine. J Nanobiotechnol. 2021; 19: 394–416.

21. Folk D, Torosian J, Hwang S, McCafferty D, Franz K. Monitoring β-secretase activity in living cells with a membrane-anchored FRET probe. Angew Chem Int Ed. 2012;51: 10795–99.
22. Kovacs G. Invited review: neuropathology of tauopathies: principles and practice. Neuropathol Appl Neurobiol. 2015; 41: 3–23.
23. Erbas-Cakmak S, Kolemen S, Sedgwick AC, Gunnlaugsson T, James TD, Yoon J, Akkaya EU. Molecular logic gates: the past, present and future, Chem Soc Rev. 2018; 47: 2228–48.
24. Wu X, Shi W, Li X, Ma H. A strategy for specific fluorescence imaging of monoamine oxidase A in living cells, Angew Chem Int Ed. 2017;56: 15319–23.
25. a) Rao L, Chi B, Ren Y, Li Y, Xu X, Wan J. A new computational protocol for accurate prediction of the protein–ligand binding structures. J Comput Chem. 2016; 37: 336 – 44; b) Wei L, Chi B, Ren Y, Rao, Wu J, Shang H, Liu JQ, Xiao YT, Ma MH, Xu X, Wan J. Conformation search across multiple-level potential-energy surfaces (CSAMP): A strategy for accurate prediction of protein–ligand binding structures. J Chem Theory Comput. 2019; 15: 4264-79.
26. Bi A, Liu M, Huang S, Zheng F, Ding J, Wu J, Tang G, Zeng W. Construction and theoretical insights into the ESIPT fluorescent probe for imaging formaldehyde in vitro and in vivo, Chem Commun. 2021; 57: 3496–9.

Figures

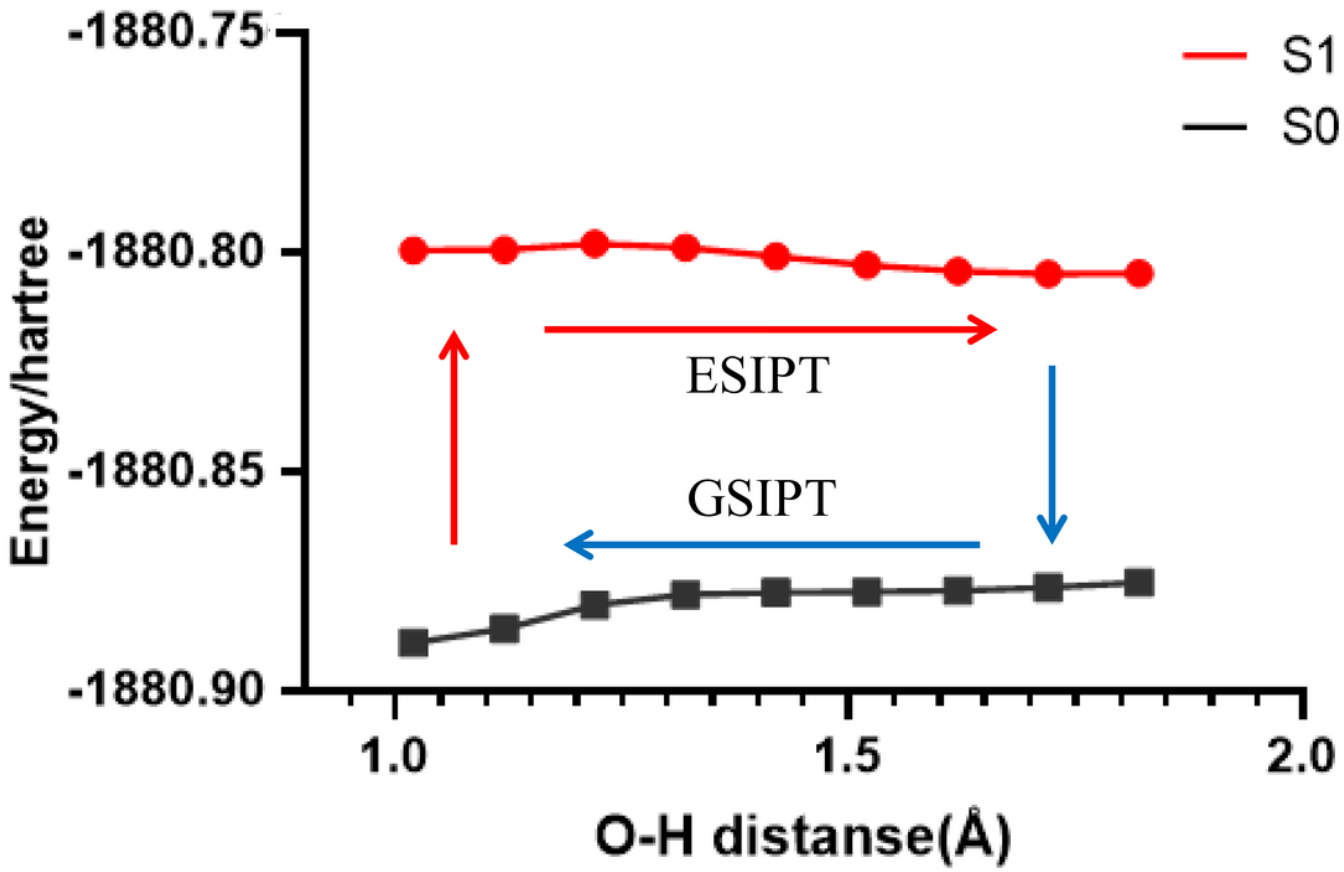

Figure 1

The calculations of mechanism of the **HBAE** fluorescence ESIPT processes.

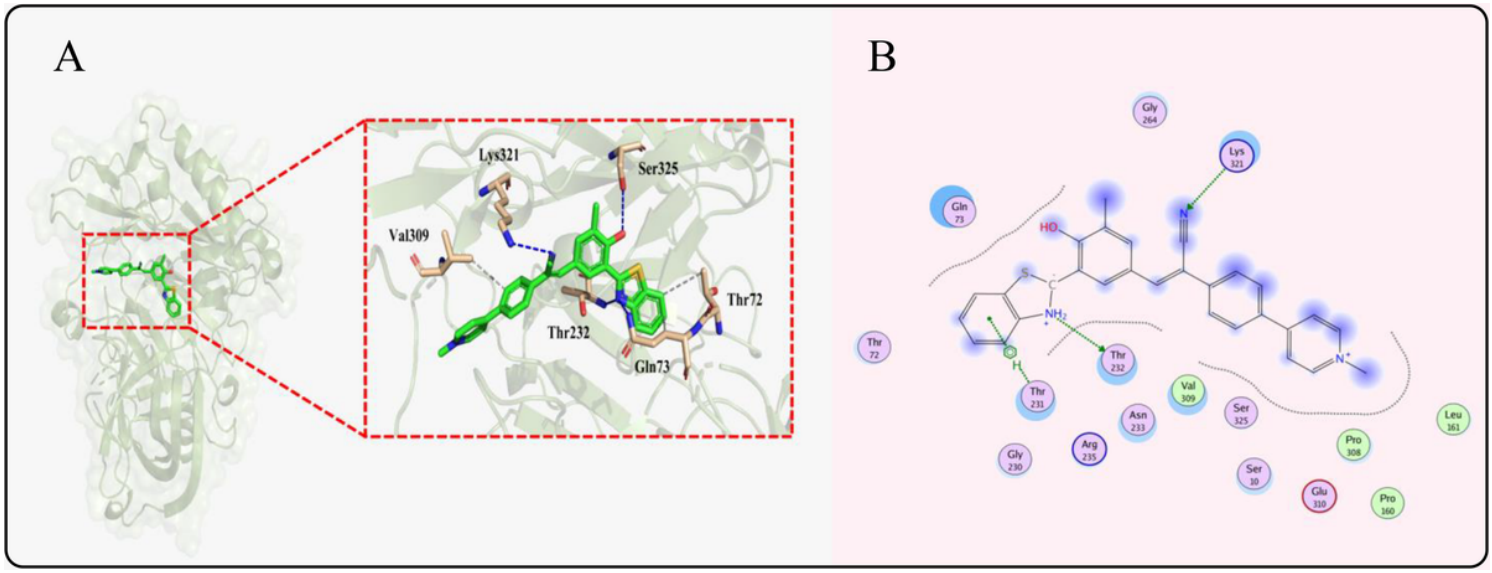

Figure 2

Illustration for the working principle of the designed NIR ratiometric fluorescent probe **HBAE** for the determination of BACE1 in neurons and mouse brain tissue slice.A: the 3D docked conformation of the BACE1 and **HBAE** of the X-ray structure of BACE1.B: the 2D docked conformation of the BACE1 and **HBAE** of the X-ray structure of BACE1 (PDB entry 5I3Y).

Figure 3

Imaging and sensing of endogenous BACE1 in four live cell lines by Alex 488-BACE1. Scale bar = 50 mm.

Figure 4

HBAE and BACE1 specific antibody (Alex fluo 488) followed by the treatment with fluorescently (Alex fluo 488) labeled secondary antibody. Scale bar = 10 mm.

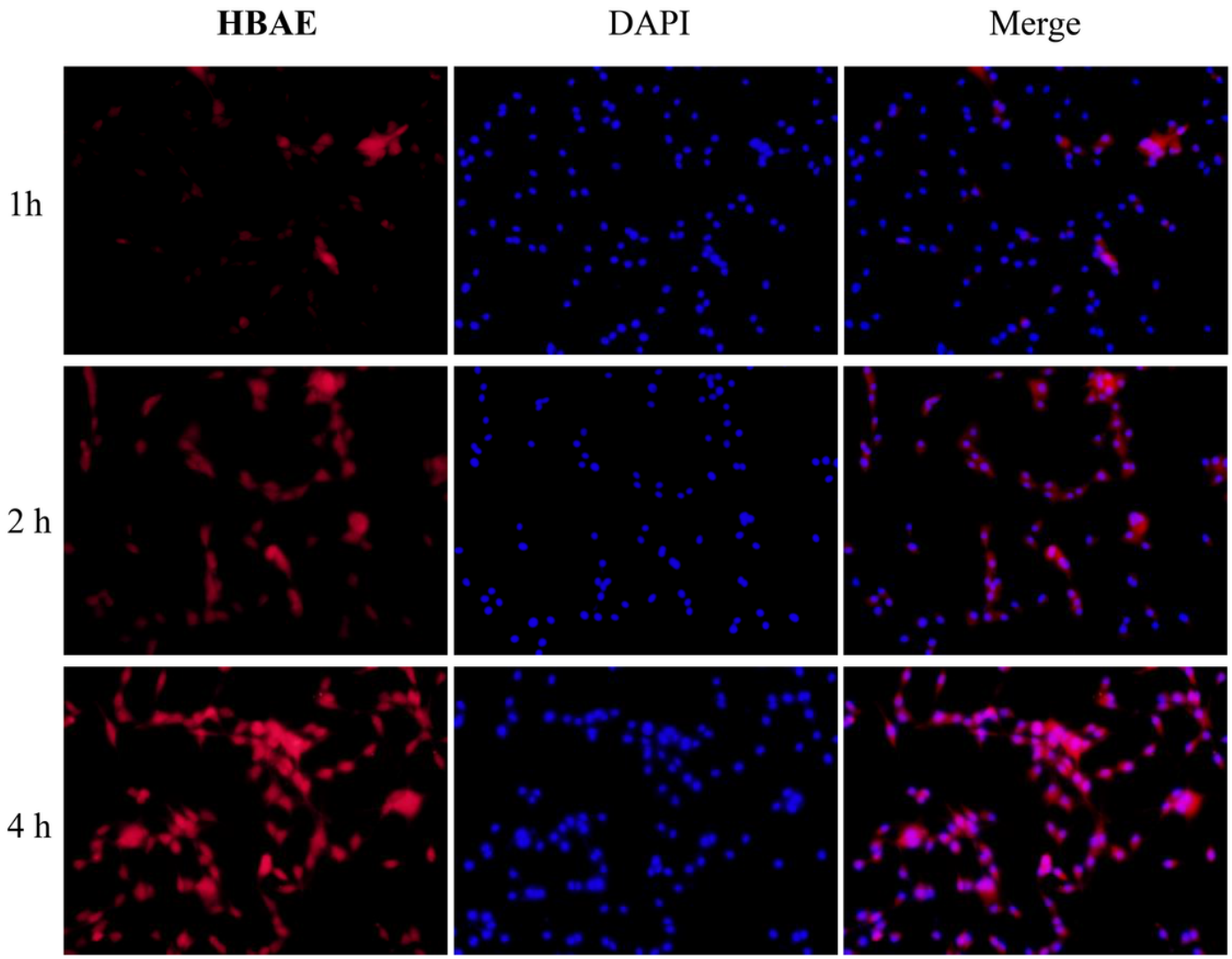

Figure 5

The penetrating blood-brain barrier ability of **HBAE** was evaluted by transwell experiment. U87-MG cells in the lower layer is obvious stained by **HBAE.** Scale bar = 50 mm.

Figure 6

In vivo mapping of BACE1 in AD model (5XFAD) mice. a. the fluorescent image at 2 h, 4 h, 8 h, 24 h after intravenous injection of 2.0 mg kg^{-1} of **HBAE** into wild-type mice and AD-model mice *in vivo*. b. the fluorescent image of ex vivo brain of wild-type mice and AD-model mice at 2 h, 4 h, 8 h, 24 h after intravenous injection of 2.0 mg kg^{-1} of **HBAE.** c. Fluorescence intensity of wild-type mice and AD-model mice in vivo at 2 h, 4 h, 8 h, 24 h after intravenous injection of 2.0 mg kg^{-1} of **HBAE**($^{***}P < 0.001$).d. Fluorescence intensity of ex vivo brain of wild-type mice and AD-model mice ($^{****}P < 0.001$).

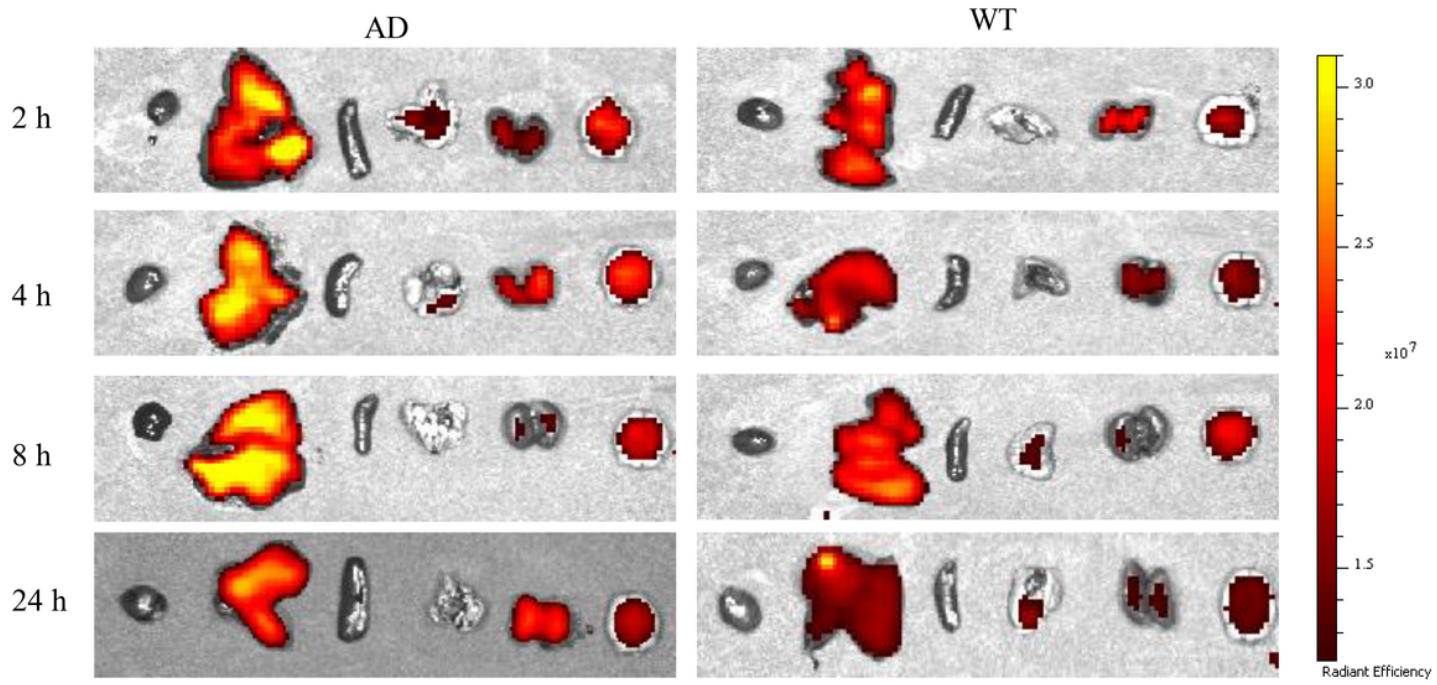

Figure 7

Ex vivo histology study of **HBAE** binding to BACE1 in AD and wild type mice. From left to right: heart, liver, spleen, lung, kidney and brain.

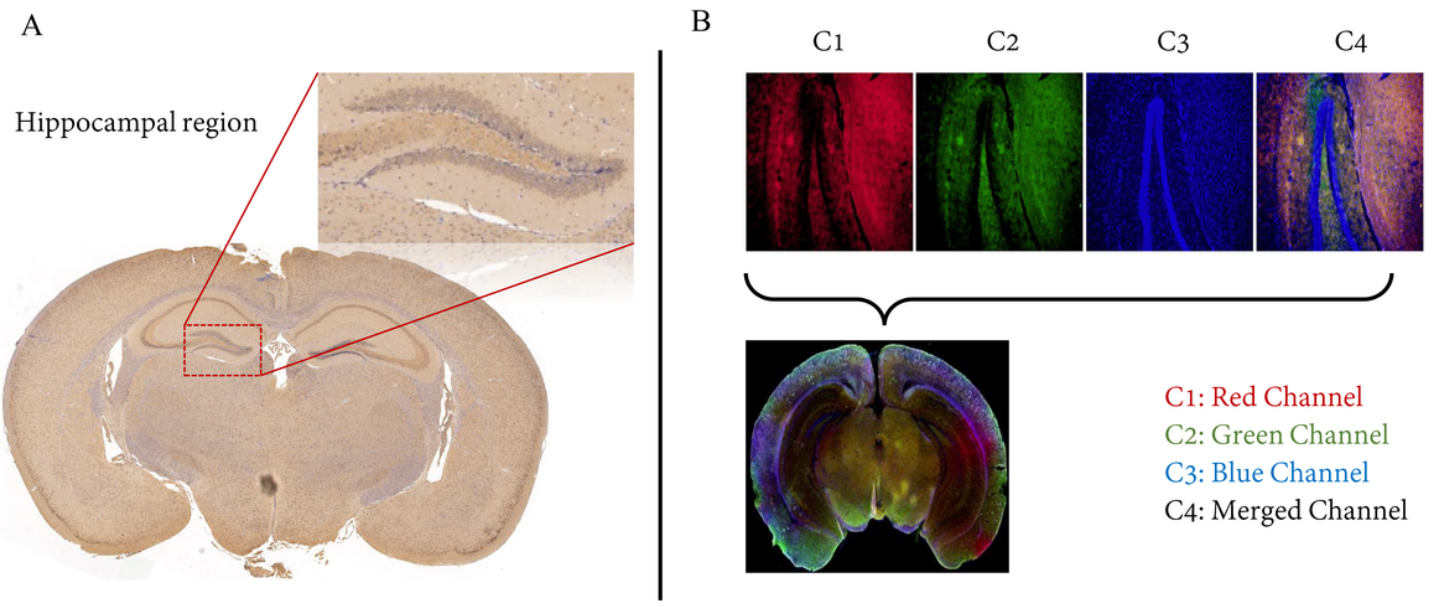

Figure 8

a. the Immunohistochemistry with the BACE1-antibody in AD mouse brain, b. the Immuno-fluorescence images of the hippocampus region in AD mouse brain tissue labelled with **HBAE** probe and Alex 488-

BACE1. Illustration for multiple regions of mouse brain slices (C_1: **HBAE**; C_2: Alex 488- BACE1; C_3: DAPI; C_4: merged).

Supplementary Files

This is a list of supplementary files associated with this preprint. Click to download.

- SupportingInformation20220510.docx